SIMPLE AND ACCURATE METHODS FOR CONVERTING CENTRIFUGE DATA INTO DRAINAGE AND IMBIBITION CAPILLARY PRESSURE CURVES

P. Forbes, Institut Français du Pétrole, 1-4 ave. de Bois Préau, 92500, Rueil-Malmaison, France.

ABSTRACT

There are various methods to reduce drainage centrifuge data to capillary pressure curves. Simple methods usually lead to poor accuracy in the results, while accurate methods, usually longer to operate, need to smooth, fit, average or force the experimental data in a given analytical form . This could be questionable and lead to significant errors in computed capillary pressure curves and consequently in computed irreducible saturation.

This paper first deals with an accurate method which is rapid to process, if the drawbacks of fitting the data in a given analytical form are accepted. The method also allows the corrected USBM wettability index to be calculated easily directly from the raw centrifuge data.

Second an accurate, very rapid and simple method is proposed. It allows to convert experimental data, even if they are noisy or few. It needs no smoothing, fitting, averaging or forcing of data, or of result, in any given form. Therefore it is believed to produce capillary pressure curves which correspond more closely to the centrifuge data than the curves which may be obtained from most other methods. The method applies to both drainage and imbibition centrifuge data. It is even simpler for imbibition.

Our first and second methods are demonstrated on both artificially generated and experimental data.

INTRODUCTION

The centrifuge has been extensively used to determine capillary pressure curves, Pc(S), for core samples since Hassler and Brunner [1] and Slobod et al. [2] formulated the theory and practice of the method. It is, however, still problematic as it requires the transformation of the centrifuge fluid production data into local saturation values. The transformation is related to assumptions on the physics of fluid displacement during centrifuging and to the inversion of a fundamental equation between local saturation S(Pc) and experimental centrifuge data [1].

The validity of physical assumptions (outflow capillary boundary condition, no cavitation, equilibrium time value, end-piece effects, homogeneity of the core, etc.) was recently reviewed by O'Meara et al. [3] and Hirasaki et al.[4]. We do not discuss these problems here but focus only on the solution of the fundamental equation.

The centrifuge method consists in measuring average saturation $\bar{S}$ versus capillary pressure Pc1 at the inlet face of a sample (Fig. 1) at equilibrium during rotation at various angular velocities ω.

From Hassler and Brunner [1] to Hermanssen et al. [5] more recently, the formulation of the mathematical link between $\bar{S}(Pc1)$ and local saturation S(Pc) can be summarized as follows: the main assumptions are that hydrostatic equilibrium is reached in each phase and that boundary condition Pc=0 is effective at the outflow face.

For drainage experiments (wetting phase saturation decreasing) capillary pressure at a position r is

$$Pc=1/2\ \Delta\rho\ \omega^2(r_2^2-r^2) \quad . \qquad (1)$$

$\Delta\rho$ is the difference between the phase densities. Average saturation is related to S by

$$\bar{S}=\frac{1}{(r_2-r_1)}\int_{r_1}^{r_2} S(r)dr \quad . \qquad (2)$$

Substituting Pc for r from (1) and eliminating $\Delta\rho\ \omega^2$ from $Pc1=\frac{1}{2}\Delta\rho\ \omega^2(r_2^2-r_1^2)$, equation (2) leads to

$$\bar{S}(Pc1)=\frac{1+\sqrt{1-B}}{2}\int_0^1 \frac{S(xPc1)}{\sqrt{1-Bx}}dx,\ B=1-(\frac{r1}{r2})^2,\ 0\le B\le 1 \quad . \qquad (3)$$

For imbibition experiments (wetting phase saturation increasing) the same equation is obtained when exchanging r_1 for r_2, $B=1-(\frac{r1}{r2})^2$, and Pc1 for Pc2 [5, 17]. For both drainage and imbibition, the problem consists therefore in inverting equation (3) to obtain $S(P_C)$ from $\bar{S}(Pc1)$, usually known as a finite number of discrete experimental values.

USUAL SOLUTIONS FOR THE CENTRIFUGE EQUATION

Numerous papers have proposed various approximate solutions to equation (3) (see for instance [6] or [7]). Solutions can be classified into two kinds : those which require both differentiation and integration and those which require differentiation only. Approximate solutions of the second kind are for instance :

$$S=S_{HB}=\bar{S}+Pc\frac{d\bar{S}}{dPc1}\ ,\ \text{Hassler and Brunner [1]}, \qquad (4)$$

$$S=S_H=\frac{2\sqrt{1-B}}{1+\sqrt{1-B}}(\bar{S}+Pc\frac{d\bar{S}}{dPc1}),\ \text{Hoffman [8]},$$

$$S=S_D=\bar{S}+\frac{2\sqrt{1-B}}{1+\sqrt{1-B}}\ Pc\frac{d\bar{S}}{dPc1}\ ,\ \text{van Domselaar [9]} \quad .$$

Such solutions can be operated rapidly, from an $\bar{S}$ dataset, using conventional differencing schemes to assess derivative $\frac{d\bar{S}}{dPc1}$ ([10], for instance). Unfortunately they are accurate only for $B\ll 1$ ($r_1\approx r_2$). Approximate solutions of the first kind are more accurate but require additional integration. This is operated numerically according to usual numerical calculus by iterative processes or operated analytically forcing the data in a given analytical form [1, 6, 7, 11 to 17]. Some solutions are accurate only for a restricted range of B or Pc values. Most are time consuming or, if they are not, could be questionable because of the choice of the analytical form which they use to fit $\bar{S}$ data. Indeed, as a common feature, the proposed methods use fitting or smoothing of $\bar{S}$ datasets or (and) fitting or averaging of computed solution S. This

is due to the fact that centrifuge equation (3) is a Voltera equation known to be ill-conditioned [5, 6, 18, 19]. It increases uncertainties on $\bar{S}$ which lead to large oscillations in solution values S. Smoothing and averaging are then used to prevent such oscillations.

Indeed the user could choose to force S or $\bar{S}$ in a given analytical form. However, the choice of the form is not contain in raw experimental data and should be supported by physical consideration, otherwise that could significantly affect the S values. Figure 2 shows local curves S(Pc) obtained from a given $\bar{S}$ dataset when the data are fit in different analytical forms [6, 17] or smoothed by the spline-fit technique [13] or when S is forced in a given form [11]. Depending on the smoothing, or fitting, the results are significantly different.

In this paper, we will first propose an approximate solution of the first kind which is rapid to operate (if the drawback of data fitting is accepted) and has a practical advantage in evaluating the USBM wettability index [20, 21, 22]. Second, a direct solution (second kind) is proposed. The second solution which is accurate for any Pc and B values and very rapid to operate on $\bar{S}$ data sets, will be preferred to the first one which could be an alternate way of interpretating the data. Both operate for drainage and forced imbibition data.

FIRST KIND SOLUTION

The following analysis refers to drainage experiments but can be conducted for imbibition as well.

In order to obtain approximate solution for equation (3), we operated in analogy with the form of true analytical solution when it exists. This is the case for B=0 [1] and B=1 [6]. In these cases equation (3) reduces to :

$$B=0,\ \bar{S}_{(Pc1)}=\int_0^1 S(xPc1)dx \text{ or } \bar{S}_{(Pc1)}=(1-0)\int_0^1 \frac{S(xPc1)}{(1-x)^0}dx\ ,$$

$$B=1,\ \bar{S}_{(Pc1)}=\frac{1}{2}\int_0^1 \frac{S(xPc1)}{\sqrt{1-x}}dx \text{ or } \bar{S}_{(Pc1)}=(1-1/2)\int_0^1 \frac{S(xPc1)}{(1-x)^{1/2}}dx$$

The last form suggests looking for a solution S_υ such as

$$\bar{S}_{(Pc1)}=(1-\upsilon)\int_0^1 \frac{S\upsilon(xPc1)}{(1-x)^\upsilon}dx \qquad (5)$$

in which υ, depending on B, has to be chosen for equation (5) reproduces initial equation (3) approximately. It is shown in Appendix A1 that for $\upsilon=\frac{1-\sqrt{1-B}}{2+\sqrt{1-B}}=\frac{r2-r1}{2r2+r1}$, the difference between equations (3) and (5) is less than 0.025, i.e. it corresponds to an error on $\bar{S}$ of less than 2.5 saturation units, whatever the B or Pc values ($0\le B\le 1$ for drainage). Figure 3a shows the variation in the maximum value of this difference versus B. Equation (5c) appears to be an excellent approximation of equation (3). It is also shown in the appendix that the difference tends to zero as S tends to the initial saturation Sd. This means that S_υ would be a very good approximation of S for lower Pc values, ($S\approx Sd$, $Pc\approx Pd$, the threshold pressure), which is a range for which S is usually obtained with poor accuracy.

Equation (5c) is an Abel equation which is inverted (see Appendix A2) using conventional calculus or a fractional derivative technique [24], leading to

$$S \approx S_\upsilon=\frac{\sin(\upsilon\pi)}{(1-\upsilon)\pi}\ \frac{d}{dPc}\left(\int_0^{Pc}\bar{S}(x)\left[\frac{x}{Pc-x}\right]^{1-\upsilon}dx\right)$$

$$\text{with}\quad \upsilon=\frac{1-\sqrt{1-B}}{2+\sqrt{1-B}}=\frac{r2-r1}{2r2+r1}\ . \qquad (6)$$

Compared to previous solutions, this one also needs integration and differentiation, but not numerical inversion of equation (3). As shown in Appendix A3, integration and differentiation can be removed, i.e. done analytically, when a subpolynomial form is used to fit $\bar{S}$ data. S_υ is then obtained as a polynomial function without any specific numerical treatment.

Integrating equation (6) leads to

$$\int_0^{Pc} S_\upsilon(x)dx=\frac{\sin(\upsilon\pi)}{(1-\upsilon)\pi}\left(\int_0^{Pc}\bar{S}(x)\left[\frac{x}{Pc-x}\right]^{1-\upsilon}dx\right). \qquad (7)$$

Using equation (7), $\int_0^{Pc} S_\upsilon(x)dx$ can be calculated directly from $\bar{S}$ values without computing local S values. Therefore the method can be used to obtain the corrected USBM wettability index [20] as simply as the uncorrected index (based on $\int_0^{Pc}\bar{S}(x)dx$ instead of $\int_0^{Pc}S(x)dx$, [21, 22]).

The method is now illustrated on artificially generated $\bar{S}$ obtained according to equation (3) for different B values and from

$$0\le Pc\le 2 : S=1;\ \ 2<Pc : S=\frac{1.5}{Pc}+0.25\ \ [6, 9, 12]\ . \qquad (8)$$

Figure 4 shows S and, for several B values, $\bar{S}$ curves and corresponding S_υ according to equation (6). The S_υ curves match the actual S curves well, whatever the B value.

Figure 5 shows the application on a polynomial fit of an experimental $\bar{S}$ dataset from Bentsen and Anli [11]. Again, results are very close to those obtained by Ayappa et al. [6] applying various methods on the same fit. The same observation can also be made in Figure 6 showing the processing of data from Glotin et al. [17].

It can be concluded that this first method yields the same result as the more accurate other methods which are longer to operate. The computed S_υ is very close to true local S curves, providing the data smoothing is convenient. Unfortunately, in actual cases the suitability of a given smoothing or fitting can not be checked as the actual S is not available (see Fig. 2). Figure 7 shows an example in which the fit fails in reconstructing the local curve. In this example data are generated from the step function:

$$0\le Pc\le 1: S=0.9;\ 1<Pc\le 4: S=0.4;\ 4<Pc: S=0.1\ . \qquad (9)$$

The data fit (continuous line) seems good, the S_υ curve is also acceptable in shape but differs significantly from the original S curve (9).

This is why another method unrelated to any preliminary smoothing or fitting is now presented.

SECOND KIND SOLUTION

As obtained by Ruth and Wong [14] from numerical computation, it can be noted in several papers that for drainage experiments, the S_{HB} approximation is lower than the exact solution, while the S_D approximation is higher [12, 23]. This is in fact always true for both drainage and imbibition and can be demonstrated analytically (Appendix B). We may therefore write

$$S_{HB}\le S\le S_D \text{ or } \bar{S}+Pc\frac{d\bar{S}}{dPc1}\le S\le \bar{S}+\frac{2\sqrt{1-B}}{1+\sqrt{1-B}}Pc\frac{d\bar{S}}{dPc1} \quad (10a)$$

or by integration (Appendix B)

$$\int_0^1 S(xPc1)dx\ge\bar{S}\ge\left(1+\frac{1-\sqrt{1-B}}{2\sqrt{1-B}}\right)\int_0^1 x^{\frac{1-\sqrt{1-B}}{2\sqrt{1-B}}}S(xPc1)\,dx \quad (10b)$$

Operating now in analogy with inequalities (10b), we proposed to approximate centrifuge equation (3) by

$$\bar{S}(Pc1)\approx(1+\alpha)\int_0^1 x^\alpha\, S(xPc1)\,dx, \text{ where } 0\le\alpha\le\frac{1-\sqrt{1-B}}{2\sqrt{1-B}}$$

according to (10b). (11)

As done previously when choosing υ, α has to be taken as a function of B in order to make (11) close enough to (3). This is obtained for $\alpha=\frac{1-\sqrt{1-B}}{1+2\sqrt{1-B}}$ (Appendix C1).

The difference between equations (11) and (3) can be demonstrated to be less than $|h_\alpha|_{max}$ [Sd-S(Pc1)], where $|h_\alpha|_{max}$ depending on B is plotted in Figure 3b (Appendix C1). According to the figure, for drainage, equation (11) would be a good approximation of (3) for $0<B\le0.7$. A possible approximation of S is therefore the solution S_α of

$$\bar{S}(Pc1)=(1+\alpha)\int_0^1 x^\alpha S_\alpha(xPc1)\,dx,\ \alpha=\frac{1-\sqrt{1-B}}{1+2\sqrt{1-B}}\ . \quad (12a)$$

This is inverted easily by differentiation as (Appendix C1):

$$S(Pc)\approx S_\alpha(Pc)=\bar{S}(Pc)+\frac{Pc}{1+\alpha}\frac{d\bar{S}}{dPc1}(Pc)$$

$0<B\le0.7$, **drainage** . (12b)

For $0.7\le B\le1$, $|h_\alpha|_{max}$ may increase by few percents and solution S_α may differ from the true S. This is illustrated in Figures 8 and 9 for artificially generated centrifuge data from

$0\le Pc\le2: S=1\ ;\ 2<Pc: S=\frac{1.5}{Pc}+0.25$

and from

$0\le Pc\le2: S=1\ ;\ 2<Pc: S=0.3$.

For such S, $\bar{S}$, $\frac{d\bar{S}}{dPc1}$ and S_α can be calculated analytically. Figures 8 and 9 show $\bar{S}$ and S_α for B= 0.1, 0.5, 0.8 and 1.0. Significant differences between the true S and S_α are observed for $0.7<B\le1$, while satisfactory agreements are obtained otherwise.

The S_α solution is accurate for B<0.7. Desirable improvements when $0.7<B\le1$ can be obtained by looking for another solution S_β which will tend to be more or less "symmetrical" to S_α with respect to S. More or less "symmetrical" means that S_β will tend to overestimate S whereas S_α underestimates S and inversely. Therefore a mere combination of S_α and S_β will lead to an accurate approximation of S. Such a S_β solution is expected by symmetrizing equation (12a), replacing $\bar{S}$ by S (lower than $\bar{S}$) and replacing S by a function related to $\bar{S}$ and lower than S. S_{HB} is known to satisfy this condition (10a) (Appendix B), so that S_β can be looked for as the solution of

$$S_\beta(Pc)=(1+\beta)\int_0^1 x^\beta\, S_{HB}(xPc)\,dx \quad (13a),$$

or as the solution of (Appendix C2)

$$\bar{S}(Pc1)=\int_0^1\left(S_\beta(xPc1)+\frac{xPc1}{1+\beta}\frac{dS_\beta}{dPc}(xPc1)\right)dx. \quad (13b)$$

Again, β is taken to make (13b) close to fundamental equation (3), leading to (Appendix C2)

$$S(Pc)\approx S_\beta(Pc)=(1+\beta)\int_0^1 x^\beta S_{HB}(xPc)dx,\ \beta=2\frac{1+2\sqrt{1-B}}{1-\sqrt{1-B}}\ . \quad (14)$$

Figures 10 and 11 show S, S_{HB}, $\bar{S}$, S_α, S_β and $\frac{S_\beta+S_\alpha}{2}$ curves for B=1.0 for the previous artificially generated $\bar{S}$ (Fig. 8, 9). Note the approximate symmetrical shape of S_α and S_β with respect to S. Note also the close agreement between S, the true solution, and $\frac{S_\beta+S_\alpha}{2}$.

For $0\le B<1$, such a close agreement was obtained using $S_{\alpha\beta}=\frac{B}{2}S_\beta+[1-\frac{B}{2}]S_\alpha$ as the approximate solution of S.

Therefore the corrected solution is summarized as

$$S_\alpha(Pc)=\bar{S}(Pc)+\frac{Pc}{1+\alpha}\frac{d\bar{S}}{dPc1}(Pc)\ ,\ \alpha=\frac{1-\sqrt{1-B}}{1+2\sqrt{1-B}}$$

$$S_\beta(Pc)=(1+\beta)\int_0^1 x^\beta\, S_{HB}(xPc)\,dx\ ,\ \beta=\frac{2}{\alpha}$$

$$S(Pc)\approx S_{\alpha\beta}=\frac{B}{2}S_\beta+[1-\frac{B}{2}]S_\alpha;\ 0\le B\le1, \textbf{ drainage} \quad (15)$$

The solution contains integration and differentiation, as do numerous solutions proposed. But this solution can be evaluated with high accuracy from

discrete $\bar{S}$ data, by using a simple differencing scheme (see [10], for other possible schemes) :

According to (15), $S_\alpha(Pc)$ is written as $S_\alpha = \frac{dPc1^{1+\alpha}\bar{S}}{dPc1^{1+\alpha}}$, while according to (A26, Appendix C2), $S_\beta(Pc)$ verifies

$$S_{HB} = \frac{dPc1\bar{S}}{dPc1} = \frac{dPc1^{1+\beta}S_\beta}{dPc1^{1+\beta}} \quad . \qquad (16)$$

Let $\{\bar{S}_i, P_i\}$ and $\{\bar{S}_{i-1}, P_{i-1}\}$ denote two successive pairs of data ($P_{i-1} < P_i$). Equations (16) lead to

$$S_{\alpha i-1/2} = \frac{P_i^{1+\alpha}\bar{S}_i - P_{i-1}^{1+\alpha}\bar{S}_{i-1}}{P_i^{1+\alpha} - P_{i-1}^{1+\alpha}} \qquad (17)$$

and $\frac{P_i\bar{S}_i - P_{i-1}\bar{S}_{i-1}}{P_i - P_{i-1}} = \frac{P_i^{1+\beta}S_{\beta i} - P_{i-1}^{1+\beta}S_{\beta i-1}}{P_i^{1+\beta} - P_{i-1}^{1+\beta}}$.

Subscripts $i-\mu$, $0 \le \mu \le 1$ refer to the value of the function at pressure $P_i - \mu\,[P_i - P_{i-1}]$.

Rearranging (17) the solution is then obtained as:

$$S_{\alpha\, i-1/2} = \frac{\bar{S}_i - [\frac{P_{i-1}}{P_i}]^{1+\alpha}\bar{S}_{i-1}}{1 - [\frac{P_{i-1}}{P_i}]^{1+\alpha}};$$

$$S_{\beta i} = [\frac{P_{i-1}}{P_i}]^{1+\beta}S_{\beta i-1} + \frac{1-[\frac{P_{i-1}}{P_i}]^{1+\beta}}{1-[\frac{P_{i-1}}{P_i}]}\left(\bar{S}_i - [\frac{P_{i-1}}{P_i}]\bar{S}_{i-1}\right);$$

$$S_{i-1/2+B/4} \approx S\alpha\beta_{i-1/2+B/4} = [1-\frac{B}{2}]S\alpha_{i-1/2} + \frac{B}{2}S_{\beta i} \qquad (18)$$

drainage, $0 \le B \le 1$, $B = 1-(\frac{r1}{r2})^2$, $\alpha = \frac{1-\sqrt{1-B}}{1+2\sqrt{1-B}} = \frac{r2-r1}{r2+2r1}$, $\beta = \frac{2}{\alpha}$

Using this scheme, solution S for the step i is obtained directly from the values of $\bar{S}$ at steps i and i-1 and from the value of S at step i-1. No iteration, smoothing, fitting, numerical integration or specific numerical treatment are needed. This produces a scheme that is easy to operate and which can process a current $\bar{S}$ dataset in less than one second on a personal computer (including plotting of input and output).

Validation

First, the applicability of the method is tested on artificially generated datasets. Figures 12 to 15 show on one hand different sets of data generated from different kinds of local S curves according to equation (3) for different B values ; on the other hand, they show the corresponding sets of $S\alpha\beta_{i-1/2+B/4}$ according to (18). The matches with initial true S are very good.

Figure 13 shows the method's capability of reproducing irregular capillary pressure curves. This is not possible for most usual methods.

The effect of the number of data points or of the pressure stepsize is illustrated in Figure 16, where S is calculated from $\bar{S}$ datasets with 2, 3, 5, 7 and 10 data. It appears that the method is not very sensitive to the number of data points, provided a lower limit of about 5 is reached.

Second the method is checked against processing of raw experimental data. As stated in the introduction, processing of experimental data could lead to oscillations in calculated S values. To prevent such oscillations we propose not to use smoothing of $\bar{S}$ or averaging of S results, but rather physical constraints such as $S_j \le S_{j-1}$ or constraints deduced from the centrifuge equation itself such as

$$S_j \le \bar{S}_j - \frac{1-\sqrt{1-B\frac{Pd}{Pc_j}}}{\sqrt{1-B\frac{Pd}{Pc_j}} - \sqrt{1-B}}[Sd-\bar{S}_j] \text{ (Appendix C3). (19)}$$

Combining such controls with the scheme (18) leads to a rapid and stable method to obtain the local S(Pc) points from experimental data.

Note that scheme (18) can be reverted leading to an expression of $\bar{S}_i$ as a function of $S\alpha\beta_{i-1/2+B/4}$, $S\alpha\beta_{i-1/2+B/4-1}$, $\bar{S}_{i-1}$ and $\bar{S}_{i-2}$. This allows the raw values of $\{S\alpha\beta_i\}$ to be changed and the corresponding effect on those of $\{\bar{S}_i\}$ to be observed immediately. This means that when we are operating on noisy data, the suitability of possible changes due to constraints (19) are immediately tested by reverting (18) to obtain the corresponding average saturation $\bar{S}$ (Fig. 17). This also means that, if for any other reason (smoothing for instance) the user wishes to change the solution given by (18) and (19), he can immediately check agreement between his changes and the experimental data. The method is interactive, immediatly linking a given $\bar{S}$ to the corresponding S or a given S to the corresponding $\bar{S}$.

Figure 17 shows the processing of noisy data from Bentsen and Anli [11] already appearing in Figure 2. Our solution is in the range of the different solutions reported by Bentsen and Anli [11], Ayappa et al. [6], Glotin et al. [17] and Skuse et al. [13]. Our solution does not present a shape as regular as the shape of the other solutions. However, as long as it does not assume any particular smooth or fit, it is believed to correspond better to the raw $\bar{S}$ dataset. The continuous line through the $\bar{S}$ data represents the transformation of our solution when equation (18) is reverted. The solution corresponds quite well to the $\bar{S}$ data.

Figures 18 and 19 present drainage data from sandstone cores from a North Sea field. Our $S\alpha\beta$ solutions are compared to the $S\upsilon$ solutions obtained when a polynomial form is used to fit data (Appendix A3). The $S\alpha\beta$ solutions are less smoothed than the $S\upsilon$ solution, but they better account for the irregularity of the $\bar{S}$ data. Moreover, the $S\alpha\beta$ solutions are obtained much more rapidly and using simpler computing.

Figure 20 displays the interpretation of data from Glotin et al. [17] and the corresponding drainage capillary pressure curve measured by mercury injection. A fair agreement between our $S_{\alpha\beta}$ solution and the mercury injection curve can be observed.

From these examples, it can be concluded that the method applies to experimental data even if these data are noisy or include irregularities. Although simple to operate, it provides accurate results accounting for detailed data distribution which, otherwise, could be lost when smoothing.

IMBIBITION

Although fundamental equation (3) applies also to forced imbibition, few papers deal with the related theory, methodology or experimental data [17, 5].

In analogy with what is observed for drainage, we expect that smoothing, fitting or averaging will lead to the same drawbacks. For instance, Hermansen et al. [5] applied an averaging procedure when oscillations take place in computed S values. Their procedure smooths the S(Pc) result which apparently becomes suitable in shape for capillary pressure curves (Fig. 21). However, when smoothed S values are used to recompute the corresponding $\bar{S}$ according to equation (3), a significant underestimation of the initial $\bar{S}$ data is obtained (Fig. 21). Indeed, in this case averaging leads to a result with a suitable shape which is infact a poorly accurate result.

To prevent such drawbacks, the same S_υ, S_α and S_β solutions proposed for drainage can be similarly developed, replacing $B=1-(\frac{r1}{r2})^2$ by $B=1-(\frac{r2}{r1})^2$.

The proposed solution is even simpler for forced imbibition, because the error due to the simplest solution, S_α, is lower than it is for drainage and fairly low whatever the B value (Fig. 3 c).

For forced imbibition an accurate approximate solution of equation (3) is therefore given by

$$S(Pc)\approx S_\alpha(Pc) = \bar{S}(Pc) + \frac{Pc}{1+\alpha}\frac{d\bar{S}}{dPc}(Pc),$$

$$\alpha = \frac{1-\sqrt{1-B}}{1+2\sqrt{1-B}} \qquad B<0, \textbf{ imbibition} \quad . \qquad (20)$$

This leads to an accurate treatment of $\bar{S}$ dataset, using the same differencing scheme already presented for drainage,

$$S_{i-1/2}\approx S_{\alpha i-1/2} = \frac{\bar{S}_i - [\frac{P_{i-1}}{P_i}]^{1+\alpha}\bar{S}_{i-1}}{1-[\frac{P_{i-1}}{P_i}]^{1+\alpha}}; \quad S_0=Sd;$$

$$\textbf{imbibition}, \ B<0, B=1-(\frac{r2}{r1})^2, \ \alpha=\frac{1-\sqrt{1-B}}{1+2\sqrt{1-B}}=\frac{r1-r2}{r1+2r2}, \ (21)$$

As for drainage, the scheme is very rapid to operate.

Figures 22 to 25 show different sets of artificial data generated from different kinds of local S curves according to equation (3) for different B values, and the corresponding sets of Sα according to (21). The matches with initial true S are still very good.

Figure 25 especially shows that irregular capillary pressure curves are also reconstructed, and not smoothed, by scheme (21).

When applying the method to experimental raw imbibition data, possible oscillations are prevented by using the following constraints equivalent to those demonstrated for drainage : $S_j \geq S_{j-1}$ for $P_j \leq P_{j-1}$

$$S_j \geq \bar{S}_j - \frac{1-\sqrt{1-B\frac{Pd}{Pc_j}}}{\sqrt{1-B\frac{Pd}{Pc_j}}-\sqrt{1-B}}[Sd-\bar{S}_j], \text{ (Appendix C3). (22)}$$

Figures 26 to 29 are some examples of applying the method to experimental data. Figure 26 shows the treatment of $\bar{S}$ data from Hermansen et al. [5] already presented in Figure 21. Our S_α solution is higher than the averaged solution found by these authors. However, the present solution is believed to be more accurate to the extend that it allows initial $\bar{S}$ data to be closely reconstructed when it is tranformed according to (3) (which is not the case for the averaged solution, Fig. 21).

In Figure 27, the S_α solution differs slightly from the solution obtained by Glotin et al. [17] when data are fit in a homographic form $\frac{a+b\,Pc}{1+c\,Pc}$. It can be noted that differences occur where the fit does not respect the initial $\bar{S}$ data (Fig. 27). Our solution is again believed to be better as it closely reproduces the data.

Figure 28 shows the application to data related to packed sand with varying wettability. The S_α solutions are very close to those obtained when we use the explicit formula proposed by Glotin et al.[17], similar to Rajan's approximation. The same observations can be made on Figure 29.

It can be concluded that the method applies to forced imbibition with the same speed and accuracy as it does to drainage.

CONCLUSION

Two methods are proposed to convert centrifuge data $\bar{S}$ into drainage or imbibition capillary pressure curves Pc(S) or S(Pc). Both are demonstrated from processing of artificially generated or experimental data. They are rapid to operate, accurate and simpler than previous methods.

The first method, related to the equation 6, in practice required the smoothing of the data in a given analytical form in order to be operated rapidly. Its drawback is linked to this smoothing, whose suitability can not be checked, exactly as in other methods using smoothing, fitting or averaging. Its advantages are that it leads to continuous capillary pressure curves, with a regular shape and a related analytical expression. It also allows the corrected USBM wettability index to be calculated directly from experimental data.

The second method, related to equations 18 and 21, leads to discrete solutions $\{S_i\}$. It is very rapid, simple and accurate. It can be operated easily on a small personal computer. It does not require iterative computing, smoothing, fitting or averaging. It allows data to be

processed even if they are noisy or irregular. It applies interactively in both ways, from $\overline{S}$ to S or from S to $\overline{S}$. In practice, this last method is observed to be very efficient and should be preferred to the first method.

In this paper we also analytically demonstrated that the Hassler and Brunner solution is always lower than the true capillary pressure curve, while the van Domselsaar solution is always higher.

All the results are obtained for both drainage and forced imbibition.

NOMENCLATURE

Latin	r	Radial distance from the centrifuge axis to a point in the centrifuged core
	r1	r at the inner core face
	r2	r at the outer core face
	Pc	Capillary pressure
	Pd	Threshold pressure
	Pc1	Pc evaluated at r1
	Pc2	Pc evaluated at r2
	S	Wetting phase saturation
	Sd	S before Pc reaches Pd
	$\overline{S}$	Average wetting phase saturation
	S_{HB}	Hassler and Brunner saturation
	S_H	Hoffman saturation
	S_D	Van Domselaar saturation
	S_υ	Approximate evaluation of S
	S_α	Approximate evaluation of S
	S_β	Approximate evaluation of S
	$S_{\alpha\beta}$	Approximate evaluation of S
	B	Dimensionless factor, $B=1-[\frac{r1}{r2}]^2$ for drainage, $B=1-[\frac{r2}{r1}]^2$ for imbibition
	x,y	Integration variables
	a_i	Parameter for the fit of $\overline{S}$ and S
	b_i	Parameter for the fit of S
Greek	ρ	Phase mass density
	$\Delta\rho$	Difference between the phase densities
	ω	Centrifuge angular velocity
	υ	Parameter related to the $S\upsilon$ solution
	α	Parameter related to the $S\alpha$ solution
	β	Parameter related to the $S\beta$ solution
	$\alpha\beta$	Parameter related to the $S_{\alpha\beta}$ solution
	Γ	Usual gamma function
	β	Usual beta function
	ε_υ	Error related to the $S\upsilon$ solution
Subscripts		
	o	Refers to the threshold pressure
	1	Refers to the inner core face
	2	Refers to the outer core face
	c	Capillary
	i, j	Counter of data or computed values
	υ	Refers to the $S\upsilon$ solution
	α	Refers to the $S\alpha$ solution
	β	Refers to the $S\beta$ solution
	$\alpha\beta$	Refers to the $S_{\alpha\beta}$ solution

AKNOWLEDGEMENTS

We thank G. Glotin with Elf Aquitaine, F. Baudoin with BEICIP and J.M. Lombard with IFP for providing experimental data to check the method.

REFERENCES

1 Hassler G.L. and Brunner E., 1945 : Trans. AIME, 160, 114-123.
2 Slobod R.L., Chambers A. and Prehn W.L., 1951 : Pet. Transac. AIME, v. 192, p. 127-134.
3 O'Meara D.J., Hirasaki G.J. and Rohan J.A., 1988: SPE paper 18296, Annual Technical Conference Houston.
4 Hirasaki G.J., O'Meara D.J. and Rohan J.A., 1988 : SPE paper 18592, Annual Technical Conference Houston.
5 Hermansen H., Eliassen O., Guo Y. and Skjaeveland S.M., 1991 : 1991 SCA Conference, London.
6 Ayappa K.G., Davis H.T., Davis E.A. et Gordon J., 1989 : AIChE Journal, V. 35, N° 3, 365-372.
7 King M.J., Narayanan K.R. and Falzone A.J., 1990 : 1990 SCA Conference, Paper 9011, 24 p. .
8 Hoffman R.N., 1963: Trans AIME, 228, p. 227-235.
9 van Domselaar H.R., 1964 : Rev. Tec. INTEVEP, V. 4, N. 1, p. 55-62.
10 Ruth D., and Wong S., 1990 : Journal of Canadian Petroleum Technology, v. 29, N. 3, p. 67-72.
11 Bentsen R.G. and Anli J., 1977 : SPE J., p. 57-64.
12 Rajan, R.R., 1986 : SPWLA Annual Logging Symp., June 9-13, p. 1-17.
13 Skuse B., Firoozabadi A.. and Ramey H.J., 1988 : SPE paper 18297, Annual Technical Conference, Houston, Oct. 2-5, p..
14 Ruth D., and Wong S., 1988 : 1988 SCA Conference, Aug 17-18, paper 8802, 9 p.
15 Nordtvedt, J.E. and Kolltveit K., 1988 : SPE unsolicited paper 19019.
16 Nordtvedt, J.E., Watson A.T., Mejia G. and Yang P., 1990 : SPE unsolicited paper 20805.
17 Glotin G. Genet J. and Klein P., 1990 : SPE paper 20502, 1990 Annual Technical Conference, New Orleans, Sept. 23-26, p. 313-324.
18 Linz P., 1969 : Comp. Journal, 12, 393-397
19 Linz P., 1982 : Treatment of Integral Equations by Numerical Methods, 123, Baker C.T.H. and Miller G.F. eds.
20 Hirasaki G.J., Rohan J.A., and Dubey S.T., 1990 : SCA Conference paper 9016., Aug. 15-16, Dallas 1990.
21 Donaldson E.C.,Thomas R.D. and Lorenz P.B., 1969 : SPE Journal March 1969, p.13-20.
22 Anderson W.G;, 1986 : Journal of Petroleum Technology, Novb. 198§, p. 1246-1262.
23 Melrose J.C., 1986 : SPWLA Annual Logging Symp., June 9-13, p. 1-21.
24 Oldham K.B. and Spanier J., 1974 : The Fractional Calculus. Theory and Applications of Differentiation and Integration to Arbitrary Order. Academic Press, New York- London, Richard Bellman ed., 234 p. .

APPENDIX

A) First kind solution

1 Formulation

Consider equation (3)

$$\bar{S}_{(Pc1)}=\frac{1+\sqrt{1-B}}{2}\int_0^1 \frac{S(xPc1)}{\sqrt{1-Bx}}dx \quad . \qquad \textbf{(A1)}$$

Adding and substracting $(1-\upsilon)\int_0^1 \frac{S_\upsilon(xPc1)}{(1-x)^\upsilon}dx$ leads to

$$\bar{S}_{(Pc1)}= \qquad \textbf{(A2)}$$

$$(1-\upsilon)\int_0^1 \frac{S_\upsilon(xPc1)}{(1-x)^\upsilon}dx - \int_0^1 S(xPc1)\left(\frac{1-\upsilon}{(1-x)^\upsilon}-\frac{1+\sqrt{1-B}}{2\sqrt{1-Bx}}\right)dx$$

Integrating by parts on the right hand term, one obtains

$$\bar{S}_{(Pc1)}=(1-\upsilon)\int_0^1 \frac{S_\upsilon(xPc1)}{(1-x)^\upsilon}dx - Pc1\int_0^1 h_\upsilon(x)\frac{dS}{dPc}(xPc1)dx$$

where $h_\upsilon(x)=\frac{\sqrt{1-Bx}-\sqrt{1-B}}{1-\sqrt{1-B}}-(1-x)^{1-\upsilon}$. **(A3)**

In order to disregard the second term on the right-hand side, we will take υ to satisfy $\int_0^1 h_\upsilon(x)dx=0$. This is obtained when we let $\upsilon=\frac{1-\sqrt{1-B}}{2+\sqrt{1-B}}$. Further evaluation of the error due to the disregarded term, has been made by numerically studying maximun and minimun values for $h_\upsilon(x)$, $0\le x\le 1$. One obtains that for drainage,

$|h_\upsilon(x)|\le 0.03\ B^{1.15}(1-B)^{0.0575}\le 0.025$ (Fig. 2).

Since $Pc\frac{dS}{dPc}\le 0$ and considering that $0\le S\le 1$, one can write

$$\left|Pc1\int_0^1 h_\upsilon(x)\frac{dS}{dPc}(xPc1)\,dx\right|$$

$$\le -0.03\,B^{1.15}(1-B)^{0.0575}\,Pc1\int_0^1 \frac{dS}{dPc}(xPc1)\,dx$$

$$\le 0.03\,B^{1.15}(1-B)^{0.0575}\,[Sd-S(Pc1)]\le 0.025 \qquad \textbf{(A4)}$$

Sd refers to the initial value of S before threshold pressure Pd is reached. Combining with (A3),

$$\bar{S}(Pc1)=(1-\upsilon)\int_0^1 \frac{S_\upsilon(xPc1)}{(1-x)^\upsilon}dx+\varepsilon_{\upsilon(Pc1)},\quad \upsilon=\frac{1-\sqrt{1-B}}{2+\sqrt{1-B}}$$

$$|\varepsilon_{\upsilon(Pc1)}|\le 0.03B^{1.15}(1-B)^{0.0575}[Sd-S(Pc1)]\le 0.025 \quad \textbf{(A5)}$$

Figure 3d also shows $|h_\upsilon(x)|_{max}$ for imbibition ($B<0$). Note that the accuracy of the approximation decreases for $B<-4$. However, in practical applications B is usually greater than -2 (see Fig. 26 to 29).

2 Inversion

Consider now solution S_υ of equation (A5), where the ε_υ function is disregarded : **(A6)**

$$\bar{S}_{(Pc1)}=(1-\upsilon)\int_0^1 \frac{S_\upsilon(xPc1)}{(1-x)^\upsilon}dx,\quad \upsilon=\frac{1-\sqrt{1-B}}{2+\sqrt{1-B}},\ 0\le\upsilon\le 1/2 \ .$$

Using fractional derivative formalism [24], equation (A6) can be rearranged as $\bar{S}_{(Pc1)}=\frac{(1-\upsilon)}{Pc1^{1-\upsilon}}\Gamma(1-\upsilon)\frac{d^{\upsilon-1}S_\upsilon}{dPc^{\upsilon-1}}(Pc1)$, where $\Gamma(\ )$ is the usual gamma function. **(A7)**

Multiplying both sides of (A7) by $\frac{Pc1^{1-\upsilon}}{(1-\upsilon)\Gamma(1-\upsilon)}$ and differentiating to fractional order $(1-\upsilon)$ with respect to Pc1,

$$S_\upsilon(Pc)=\frac{1}{(1-\upsilon)\Gamma(1-\upsilon)}\frac{d^{1-\upsilon}\,[Pc1^{1-\upsilon}\bar{S}]}{dPc1^{1-\upsilon}}(Pc),$$

and rewriting from the definition of fractional derivative and of the gamma function,

$$S_\upsilon(Pc)=\frac{\sin(\upsilon\pi)}{(1-\upsilon)\pi}\frac{d}{dPc}\left(\int_0^{Pc}\bar{S}(x)\,[\frac{x}{Pc-x}]^{1-\upsilon}dx\right) \qquad \textbf{(A8a)}$$

or

$$S_\upsilon(Pc)=\frac{\sin(\upsilon\pi)}{(1-\upsilon)\pi}\frac{1}{Pc}\left(\int_0^{Pc}\frac{dPc1\bar{S}}{dPc1}(x)\,[\frac{x}{Pc-x}]^{1-\upsilon}dx\right) \qquad \textbf{(A8b)}$$

or integrating with respect to Pc,

$$\int_0^{Pc}S_\upsilon(x)dx=\frac{\sin(\upsilon\pi)}{(1-\upsilon)\pi}\left(\int_0^{Pc}\bar{S}(x)\,[\frac{x}{Pc-x}]^{1-\upsilon}dx\right) \qquad \textbf{(A8c)}$$

The same results can be obtained by conventional calculus by noting that, for any Pc or y,

$$\frac{\pi}{\sin(\upsilon\pi)}=\int_y^{Pc}\frac{1}{(x-y)^\upsilon(Pc-x)^{1-\upsilon}}dx \ . \qquad \textbf{(A9)}$$

Multiplying both sides of (A9) by $\int_0^{Pc}S_\upsilon(x)\,dx$, rearranging the right-hand term as a double integral and combining with (A6) gives (A8c). (A8a) and (A8b) can be then deduced by differentiation with respect to Pc.

3 Calculation

Using equation (A8a), S_υ can be found analytically, provided $\bar{S}$ is expressed in an appropriate form as:

$\bar{S}(Pc1)=Sd,\ Pc1\le Pd$; **(A10)**

$$\bar{S}(Pc1) = Sd + \left[\frac{Pc1-Pd}{Pc1}\right]^{1-\upsilon} \Sigma_i\ a_i\ [Pc1-Pd]^i\ ,\ Pd < Pc1.$$

Substituting in (A8a), the usual beta function β appears and S_υ is obtained as

$S_\upsilon(Pc) = Sd,\ Pc \le Pd$;

$$S_\upsilon(Pc) = Sd + \Sigma_i b_i\ a_i [Pc-Pd]^i\ ,\ Pd < Pc. \qquad \textbf{(A11)}$$

$$b_i = \frac{1}{[1-\upsilon]\ \beta(1+i,1-\upsilon)}$$

The relation to the beta function can even be removed, for instance when we restrict i to be **(A12)**

- i=n, a positive integer, giving $b_i = b_{i-1}\frac{i+1-\upsilon}{i}$, $b_o = 1$
- or i = n -1+ υ, giving $b_i = b_{i-1}\frac{i+1-\upsilon}{i}$, $b_{\upsilon-1} = \frac{\sin(\upsilon\ \pi)}{(1-\upsilon)\ \pi}$

Finally, using (A12) we merely need to fit the values of a_i on $\bar{S}$ datasets according to (A10), in order to obtain an analytical expression for S_υ according to (A11).

B) $S_{HB} \le S \le S_D$

Consider equation (3). When adding and substracting

$$(1+\alpha)\int_0^1 x^\alpha\ S(xPc1)\ dx :\ \bar{S}(Pc1) = (1+\alpha)\int_0^1 x^\alpha S(xPc1)\ dx$$

$$-\int_0^1 S(xPc1)\left((1+\alpha)x^\alpha - \frac{1+\sqrt{1-B}}{2\sqrt{1-Bx}}\right)dx\ . \qquad \textbf{(A13)}$$

Integrating by parts on the right-hand term, one obtains

$$\bar{S}(Pc1) = (1+\alpha)\int_0^1 x^\alpha S(xPc1)dx - Pc1\int_0^1 h_\alpha(x)\frac{dS}{dPc}(xPc1)dx$$

$$\text{where } h_\alpha(x) = \frac{\sqrt{1-Bx}-\sqrt{1-B}}{1-\sqrt{1-B}} - x^{1+\alpha} \qquad \textbf{(A14)}$$

Transforming the variable from x to $\frac{x}{Pc1}$ in the first integral of equation (A13) we find

$$\bar{S}(Pc1) = \frac{1+\alpha}{Pc1^{1+\alpha}}\int_0^{Pc1} x^\alpha\ S(x)\ dx$$

$$-\int_0^1 S(xPc1)\left([1+\alpha]x^\alpha - \frac{1+\sqrt{1-B}}{2\sqrt{1-Bx}}\right)dx\ . \qquad \textbf{(A15)}$$

Multiplying by $Pc1^{1+\alpha}$ and taking the derivative of both sides with respect to Pc1, using Leibnizt's rule for differentiating an integral,

$$\frac{dPc1^{1+\alpha}\,\bar{S}}{dPc1}(Pc1) = [1+\alpha]\ Pc1^\alpha\ S(Pc1)$$

$$-Pc1^{1+\alpha}\int_0^1 x\left([1+\alpha]x^\alpha - \frac{1+\sqrt{1-B}}{2\sqrt{1-Bx}}\right)\frac{dS}{dPc}(xPc1)\ dx$$

$$-[1+\alpha]Pc1^\alpha\int_0^1 S(xPc1)\left([1+\alpha]x^\alpha - \frac{1+\sqrt{1-B}}{2\sqrt{1-Bx}}\right)dx\ . \textbf{(A16)}$$

Integrating by parts in the last term and rearranging

$$\frac{dPc1^{1+\alpha}\,\bar{S}}{dPc1}(Pc1) = [1+\alpha]\ Pc1^\alpha\ S(Pc1)$$

$$-[1+\alpha]\ Pc1^{1+\alpha}\int_0^1 g_\alpha(x)\frac{dS}{dPc}(xPc1)dx \qquad \textbf{(A17)}$$

$$\text{where } g_\alpha(x) = \frac{1-\sqrt{1-Bx}}{1-\sqrt{1-B}} - \frac{x}{1+\alpha}\frac{1+\sqrt{1-B}}{2\sqrt{1-Bx}}$$

$$= -\frac{1}{1+\alpha}\frac{1-\sqrt{1-Bx}}{2\sqrt{1-Bx}}\frac{1-[1+2\alpha]\sqrt{1-Bx}}{1-\sqrt{1-B}}\ .$$

Expansion of the left-side derivative and division of both sides by $[1+\alpha]\ Pc1^\alpha$ gives

$$S(Pc) = \bar{S}(Pc) + \frac{Pc}{1+\alpha}\frac{d\bar{S}}{dPc1}(Pc) + Pc\int_0^1 g_\alpha(x)\frac{dS}{dPc}(xPc)\ dx$$

$$\text{where } g_\alpha(x) = -\frac{1}{1+\alpha}\frac{1-\sqrt{1-Bx}}{2\sqrt{1-Bx}}\frac{1-[1+2\alpha]\sqrt{1-Bx}}{1-\sqrt{1-B}},\quad \alpha > -1 \qquad \textbf{(A18)}$$

Note that equations (A14) and (A18) are equivalent to centrifuge equation (3) for any α higher than -1.

Consider now $g_\alpha(x)$ for $\alpha = 0$ and for $\alpha = \frac{1-\sqrt{1-B}}{2\sqrt{1-B}}$

$$g_0(x) = -\frac{[1-\sqrt{1-Bx}]^2}{2\sqrt{1-Bx}}\frac{1}{1-\sqrt{1-Bx}} \quad \text{and}$$

$$g_{\frac{1-\sqrt{1-B}}{2\sqrt{1-B}}}(x) = \frac{1-\sqrt{1-Bx}}{B}[\sqrt{1-Bx}-\sqrt{1-B}]\ . \qquad \textbf{(A19)}$$

For drainage, since $0 \le B \le 1$ we find

$$g_0(x) \le 0 \text{ and } g_{\frac{1-\sqrt{1-B}}{2\sqrt{1-B}}}(x) \ge 0\ ,\ 0 \le x \le 1.$$

Similarly for imbibition, $B<0$ leads to

$$g_0(x) \ge 0 \text{ and } g_{\frac{1-\sqrt{1-B}}{2\sqrt{1-B}}}(x) \le 0\ ,\ 0 \le x \le 1.$$

According to $\frac{dS}{dPc} \le 0$, for both drainage ($Pc \ge 0$) and imbibition ($Pc \le 0$) we obtain $Pc \int_0^1 g_0(x) \frac{dS}{dPc}(xPc)dx \le 0$

and $Pc \int_0^{\frac{1-\sqrt{1-B}}{2\sqrt{1-B}}} g_{\frac{1-\sqrt{1-B}}{2\sqrt{1-B}}}(x) \frac{dS}{dPc}(xPc)\,dx \ge 0$. **(A20)**

Combining (A20) with (A18) for $\alpha=0$ and for $\alpha=\frac{1-\sqrt{1-B}}{2\sqrt{1-B}}$

$$\bar{S} + Pc\frac{d\bar{S}}{dPc1} \le S \le \bar{S} + \frac{2\sqrt{1-B}}{1+\sqrt{1-B}} Pc\frac{d\bar{S}}{dPc1}$$

or $S_{HB} \le S \le S_D$ **(A21a)**

Rearranging : $\frac{dPc1\bar{S}}{dPc1} \le S$ and **(A21b)**

$$S \le \frac{2\sqrt{1-B}}{1+\sqrt{1-B}} Pc1^{\frac{\sqrt{1-B}-1}{2\sqrt{1-B}}} \frac{d}{dPc1}\left(Pc1^{\frac{1+\sqrt{1-B}}{2\sqrt{1-B}}} \bar{S} \right)$$

(use -Pc2 instead of Pc1 for imbibition)

or $\frac{dPc1\bar{S}}{dPc1} \le S$ and

$$\frac{1+\sqrt{1-B}}{2\sqrt{1-B}} Pc1^{\frac{1-\sqrt{1-B}}{2\sqrt{1-B}}} S \le \frac{d}{dPc1}\left(Pc1^{\frac{1+\sqrt{1-B}}{2\sqrt{1-B}}} \bar{S} \right).$$

Integrating with respect to Pc1 and replacing the variable Pc1 by xPc1, $\int_0^1 S(xPc1)\,dx \ge \bar{S}$ and

$$\bar{S} \ge \frac{1+\sqrt{1-B}}{2\sqrt{1-B}} \int_0^1 x^{\frac{1-\sqrt{1-B}}{2\sqrt{1-B}}} S(xPc1)\,dx .$$ **(A21c)**

C) Second kind solution

1 S_α approximation

We operate on equation (A14) exactly as previously on equation (A3). In order to disregard the second integral, α is taken to satisfy $\int_0^1 h_\alpha(x)dx=0 : \alpha=\frac{1-\sqrt{1-B}}{1+2\sqrt{1-B}}$. Using this expression for α and disregarding the second integral in equation (A14) an approximate solution of equation (3) is obtained as $S\alpha$:

$$\bar{S}(Pc1)=(1+\alpha)\int_0^1 x^\alpha S_\alpha(xPc1)\,dx, \quad \alpha=\frac{1-\sqrt{1-B}}{1+2\sqrt{1-B}} .$$ **(A22)**

The magnitude of the error introduced by approximation is assessed numerically by studying the maximun value for $|h_\alpha(x)|$. Figure 3 shows this value $|h_\alpha|_{max}$ as a function of B (drainage) or $\frac{-B}{1-B}$ (imbibition).

Since $Pc\frac{dS}{dPc} \le 0$ and considering that $0 \le S \le 1$, we can write for the integral disregarded between equation (A14) and equation (A22) :

$$|Pc1 \int_0^1 h_\alpha(x)\frac{dS}{dPc}(xPc1)dx| \le |h_\alpha|_{max}[Sd-S(Pc1)] .$$ **(A23)**

This means that equation (A22) will be a good approximation of centrifuge equation (3 or A14) when $|h_\alpha|_{max}$ is fairly low. According to Figure 2 this will be the case for $0<B\le 0.7$ (drainage) and $B<0$ (imbibition).

Note that equation (A22) has been inverted in Appendix B and that the approximate solution is given by :

$$S_\alpha(Pc) = \bar{S}(Pc) + \frac{Pc}{1+\alpha}\frac{d\bar{S}}{dPc1}(Pc) , \alpha=\frac{1-\sqrt{1-B}}{1+2\sqrt{1-B}}$$ **(A24)**

For $0.7<B\le 1$, accuracy of the S_α approximation can be poor. The correction below is proposed.

2 S_β correction

Inversion of the equation (13a)

Consider the equation (13) $S_\beta(Pc)=(1+\beta)\int_0^1 x^\beta S_{HB}(xPc)dx$.

Replacing x with $\frac{x}{Pc}$ and multiplying by $Pc1^{1+\beta}$ yields

$$Pc1^{1+\beta} S_\beta(Pc) = (1+\beta)\int_0^{Pc} x^\beta S_{HB}(x)\,dx .$$ **(A25)**

Differentiating both sides with respect to Pc and dividing by $(1+\beta)\,Pc1^\beta$ gives **(A26)**

$$S_\beta(Pc)+\frac{Pc}{1+\beta}\frac{dS_\beta}{dPc}(Pc) = S_{HB}(Pc) = \frac{dPc1\bar{S}}{dPc1}(Pc).$$

Integrating with respect to Pc, one obtains

$$Pc1\,\bar{S}(Pc1)=\int_0^{Pc}\left(S_\beta(x) + \frac{x}{1+\beta}\frac{dS_\beta}{dPc}(x)\right)dx .$$ **(A27)**

Replacing x by x Pc1 leads to equation (13b)

$$\bar{S}(Pc1)\int_0^1\left(S_\beta(xPc1) + \frac{xPc1}{1+\beta}\frac{dS_\beta}{dPc}(xPc1)\right)dx .$$ **(A28)**

Choice of β value

Centrifuge equation (3) is rearranged on the form of (A28) when we add and subtract

$$\int_0^1 \left(S(xPc1) + \frac{xPc1}{1+\beta} \frac{dS}{dPc}(xPc1) \right) dx \ :$$

$$\bar{S}(Pc1) = \int_0^1 \left(S(xPc1) + \frac{xPc1}{1+\beta} \frac{dS}{dPc}(xPc1) \right) dx$$

$$+ \int_0^1 S(xPc1) \left(\frac{1+\sqrt{1-B}}{2\sqrt{1-Bx}} - 1 \right) dx - \int_0^1 \frac{xPc1}{1+\beta} \frac{dS}{dPc}(xPc1) dx. \quad \textbf{(A29)}$$

Integrating by parts the second term of the right-hand side, one obtains

$$\bar{S}(Pc1) = \int_0^1 \left(S(xPc1) + \frac{xPc1}{1+\beta} \frac{dS}{dPc}(xPc1) \right) dx$$

$$- Pc1 \int_0^1 h_\beta(x) \frac{dS}{dPc}(xPc1)\, dx, \qquad \textbf{(A30)}$$

where $h_\beta(x) = \frac{1-\sqrt{1-Bx}}{1-\sqrt{1-B}} - \frac{\beta}{1+\beta} x$.

As previously, for β satisfying $\int_0^1 h_\beta(x)dx = 0$, the second integral is disregarded in (A30) leading to **(A31)**

$$S(Pc) \approx S_\beta(Pc) = (1+\beta) \int_0^1 x^\beta S_{HB}(xPc)dx, \quad \beta = 2\frac{1+2\sqrt{1-B}}{1-\sqrt{1-B}} = 2/\alpha$$

3 Computing on raw experimental data

Converting raw $\bar{S}$ data into S, according to equation (3) or equivalent equations can generate oscillations due to poor accuracy in measured data. Such oscillations are usually prevented by smoothing, fitting or averaging which are related to possible drawbacks (see text). Here, oscillations are prevented by forcing solution S to satisfy conditions included in the centrifuge equation itself.

For drainage, $\bar{S}$ data are usually sorted in increasing order of Pc1, while for imbibition they are sorted in decreasing order of Pc1 :
drainage $\{\bar{S}_i, P_i; P_i \geq P_{i-1}\}$, imbibition $\{\bar{S}_i, P_i; P_i \leq P_{i-1}\}$.
Since $\frac{dS}{dPc}(Pc) \leq 0$, a trivial constraint is $S_j \leq S_{j-1}$ for drainage and $S_j \geq S_{j-1}$ for imbibition.

A second constraint is obtained when we split equation (3) into the following two terms : **(A32)**

$$\bar{S}(Pc1) = \frac{1+\sqrt{1-B}}{2} \int_0^{\frac{Pd}{Pc1}} \frac{S(xPc1)}{\sqrt{1-Bx}} dx + \frac{1+\sqrt{1-B}}{2} \int_{\frac{Pd}{Pc1}}^1 \frac{S(xPc1)}{\sqrt{1-Bx}} dx.$$

Since S is constant, Sd, for $Pc \leq Pd$, the first integral is

$$\frac{1-\sqrt{1-B\frac{Pd}{Pc1}}}{1-\sqrt{1-B}} Sd.$$

For drainage, $S(xPc1) \geq S(Pc1)$, therefore yielding **(A33)**

$$\bar{S}(Pc1) \geq \frac{1-\sqrt{1-B\frac{Pd}{Pc1}}}{1-\sqrt{1-B}} Sd + \frac{1+\sqrt{1-B}}{2} \int_{\frac{Pd}{Pc1}}^1 \frac{S(Pc1)}{\sqrt{1-Bx}} dx \ .$$

Integrating and rearranging

$$S(Pc1) \leq \bar{S}(Pc1) - \frac{1-\sqrt{1-B\frac{Pd}{Pc1}}}{\sqrt{1-B\frac{Pd}{Pc1}} - \sqrt{1-B}} [Sd - \bar{S}(Pc1)] \ . \ \textbf{(A34)}$$

This leads to

$$S_j \leq \bar{S}_j - \frac{1-\sqrt{1-B\frac{Pd}{Pc_j}}}{\sqrt{1-B\frac{Pd}{Pc_j}} - \sqrt{1-B}} [Sd - \bar{S}_j] \quad . \quad \textbf{(A35)}$$

Similarly, for imbibition we obtain

$$S_j \geq \bar{S}_j - \frac{1-\sqrt{1-B\frac{Pd}{Pc_j}}}{\sqrt{1-B\frac{Pd}{Pc_j}} - \sqrt{1-B}} [Sd - \bar{S}_j] \quad . \quad \textbf{(A36)}$$

FIGURES

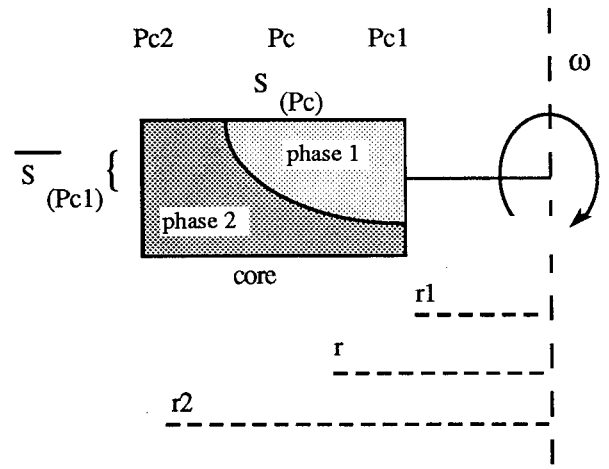

Figure 1 : Scheme of the centrifuge method.

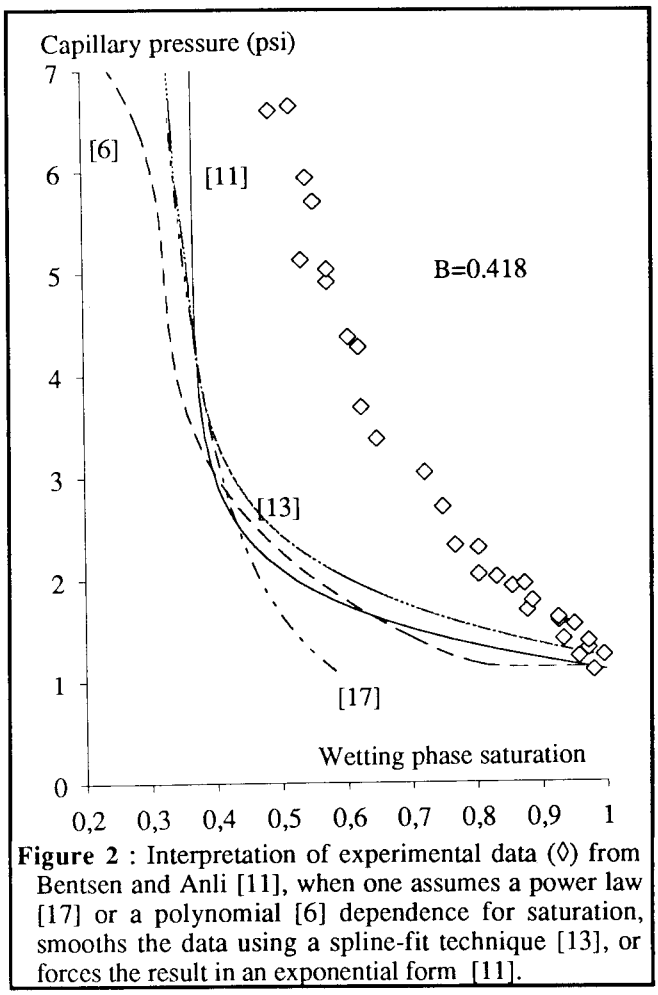

Figure 2 : Interpretation of experimental data (◊) from Bentsen and Anli [11], when one assumes a power law [17] or a polynomial [6] dependence for saturation, smooths the data using a spline-fit technique [13], or forces the result in an exponential form [11].

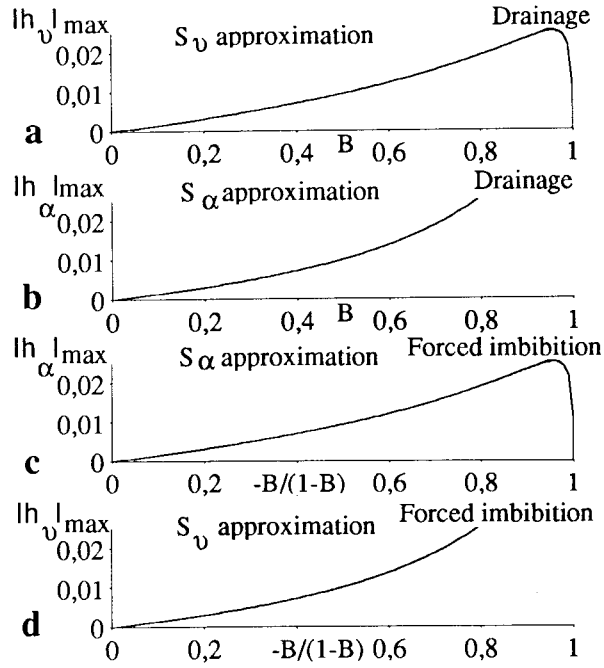

Figure 3 : Maximun error on $\overline{S}$ when we change centrifuge equation (3), in equation (5c) for drainage or imbibition [a, d], in equation (12a) for drainage [3b] and in equation (12a) for imbibition [3c].

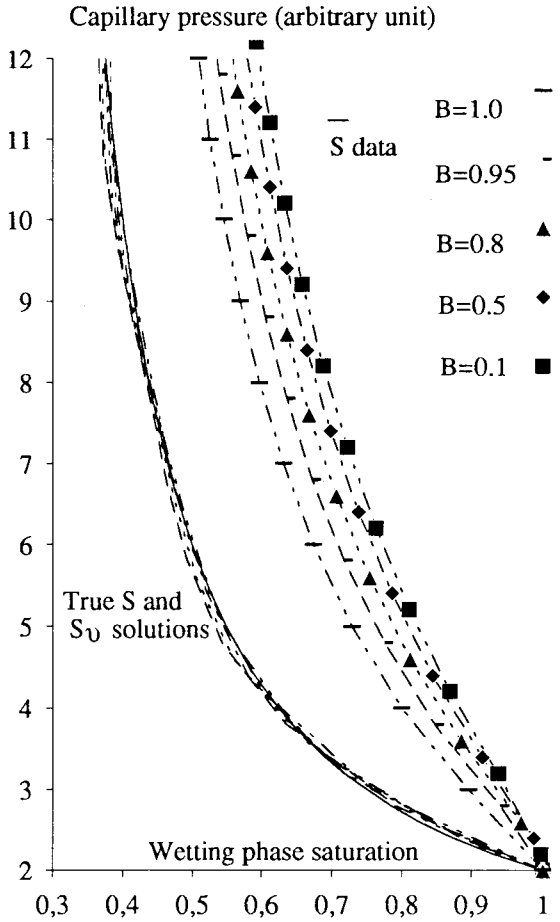

Figure 4 : Interpretation of artificially generated data. Points represent datasets generated for different B values, according to the equation (3) and assuming the capillary pressure curve is (continuous line) 0≤Pc≤2: S=1; 2<Pc: S=0.25 + 1.5/Pc . Dashed lines show data fits and the corresponding S_υ approximations.

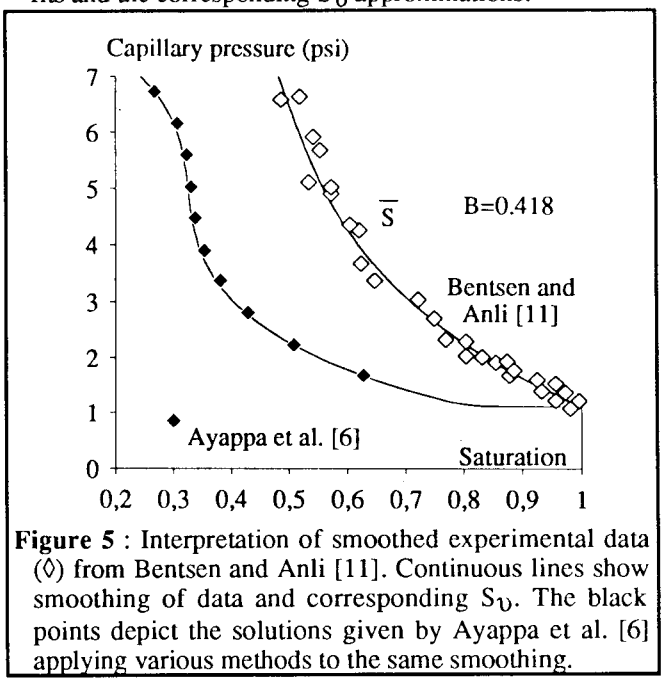

Figure 5 : Interpretation of smoothed experimental data (◊) from Bentsen and Anli [11]. Continuous lines show smoothing of data and corresponding S_υ. The black points depict the solutions given by Ayappa et al. [6] applying various methods to the same smoothing.

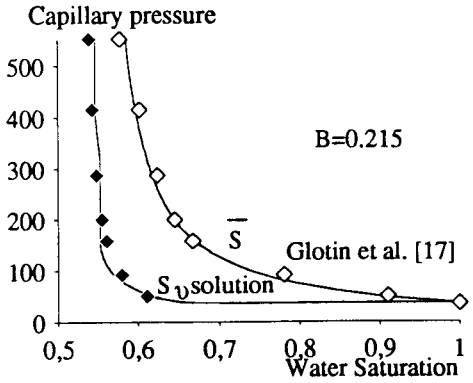

Figure 6 : Interpretation of smoothed experimental data (◊) from Glotin et al. [17] (limestone). Continuous lines show smoothing of data and corresponding S_υ. Black points depict the solution given by Glotin et al. [17] when data are forced in a power law dependence.

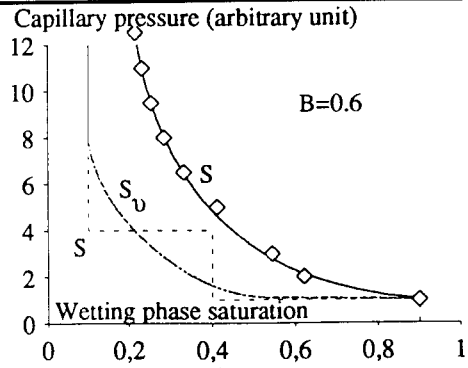

Figure 7 : Interpretation of artificially data (◊) generated for : 0≤Pc≤1 : S=0.9; 1<Pc≤4 : S=0.4; 4<Pc : S=0.1 The continuous line depicts the subpolynomial fit of the data (see text). The thick dashed line is corresponding S_υ and the light dashed line the initial step function.

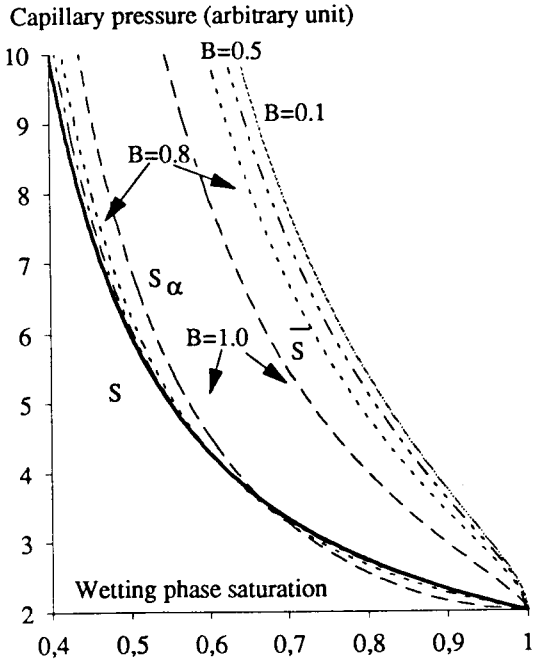

Figure 8 : Interpretation of artificially generated data. The higher lines represent data generated for different B values according to equation (3) and assuming the capillary pressure curve is (thick line) 0≤Pc≤2: S=1; 2<Pc: S=0.25 + 1.5/Pc. The lower lines show the corresponding S_α approximation (see text).

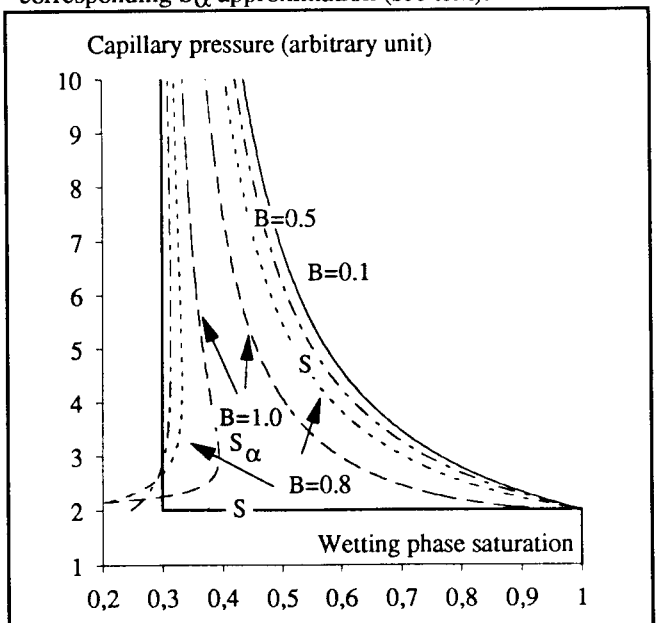

Figure 9 : Interpretation of artificially generated data. The higher lines represent data generated for different B values according to equation (3) and assuming the capillary pressure curve is (thick line) 0≤Pc≤2 : S=1 ; 2<Pc : S=0.3. The lower lines show the corresponding S_α approximation (see text).

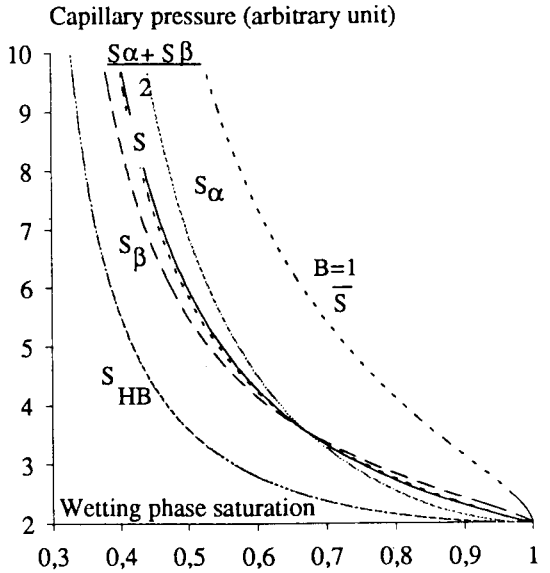

Figure 10 : Interpretation of artificially generated data. The higher line represents data generated for B=1 according to equation (3) and assuming the capillary pressure curve is (thick line) 0≤Pc≤2: S=1; 2<Pc: S=0.25 +1.5/Pc. The lower lines show corresponding S_{HB} S_α, S_β and $(S_\alpha+S_\beta)/2$ approximations (see text).

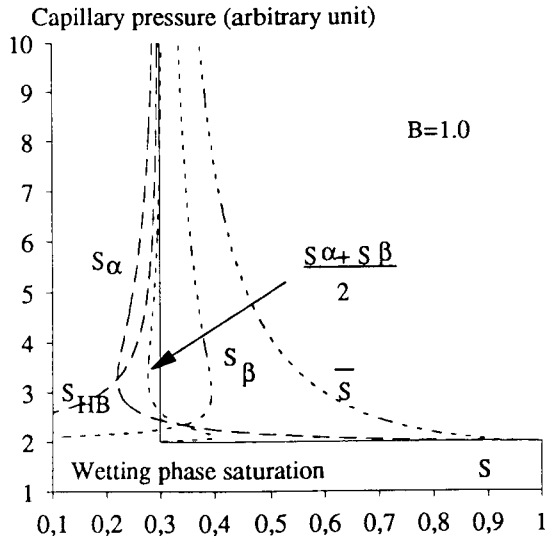

Figure 11 : Interpretation of artificially generated data. The higher line represents data generated for B=1 according to the equation (3) and assuming the capillary pressure curve is (thick line) 0≤Pc≤2: S=1; 2<Pc: S=0.3. The lower lines show corresponding S_{HB} S_α, S_β and $(S_\alpha+S_\beta)/2$ approximations (see text).

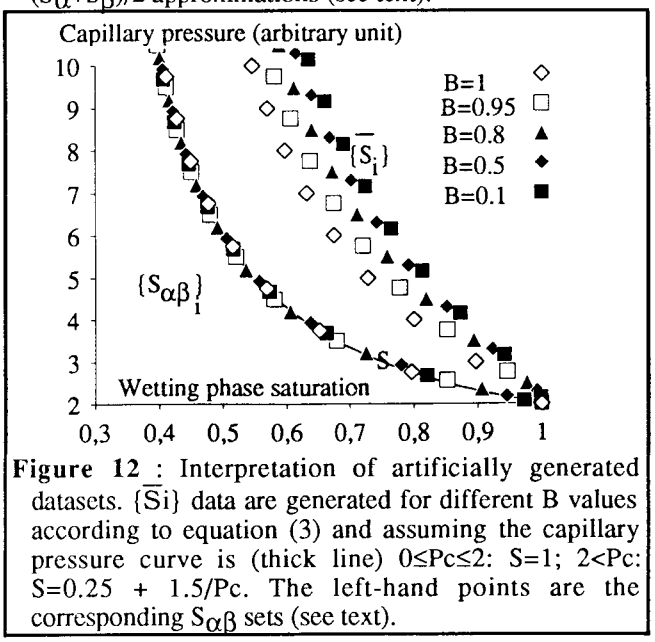

Figure 12 : Interpretation of artificially generated datasets. $\{\bar{S}i\}$ data are generated for different B values according to equation (3) and assuming the capillary pressure curve is (thick line) 0≤Pc≤2: S=1; 2<Pc: S=0.25 + 1.5/Pc. The left-hand points are the corresponding $S_{\alpha\beta}$ sets (see text).

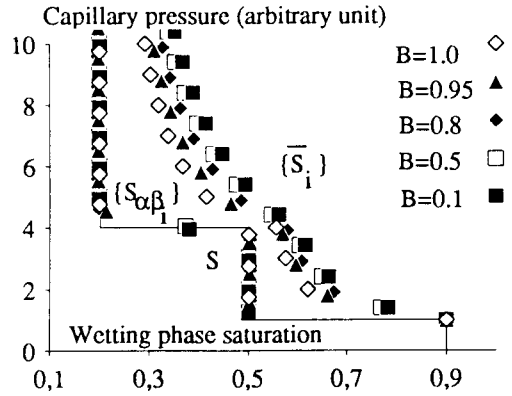

Figure 13 : Interpretation of artificially generated datasets. $\{\bar{S}i\}$ data are generated for different B values according to equation (3) for a step function (continuous line), 0≤Pc≤1: S=0.9; 1<Pc≤4 : S=0.5; 4<Pc: S=0.2. The left-hand points are corresponding $S_{\alpha\beta}$ sets.

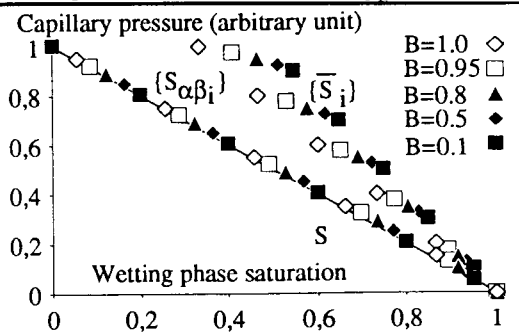

Figure 14 : Interpretation of artificially generated datasets. $\{\bar{S}i\}$ data are generated for different B values according to equation (3), for S=1-Pc (continuous line). The left-hand points are the corresponding $S_{\alpha\beta}$ sets.

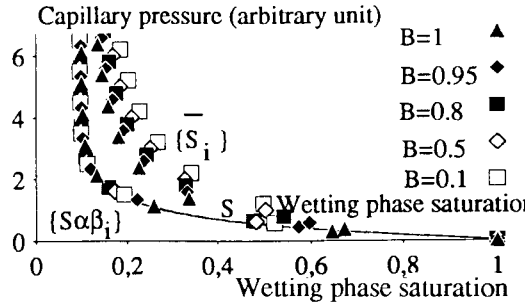

Figure 15 : Interpretation of artificial datasets. $\{\bar{S}i\}$ data are generated for different B according to equation (3), for $S=0.1+0.9\ e^{-\frac{Pc-0.05}{0.6}}$ (continuous line). The left-hand points are corresponding $S_{\alpha\beta}$ sets.

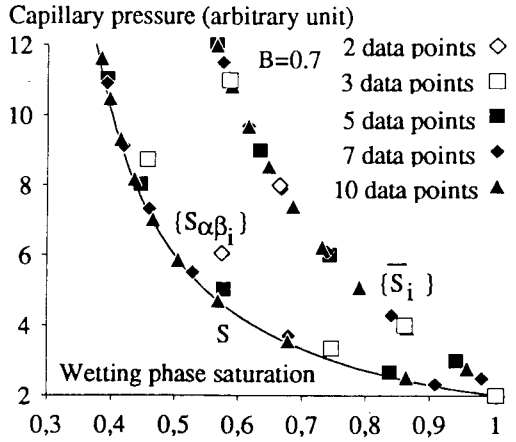

Figure 16 : Effect of number of data points and stepsize. The right-hand points represent sets of different numbers of data (and different stepsize values) generated for B=0.7 according to equation (3) and assuming the capillary pressure curve is (thick line) 0≤Pc≤2: S=1; 2<Pc: S=0.25 + 1.5/Pc. The left-hand points are corresponding $S_{\alpha\beta}$ sets (see text).

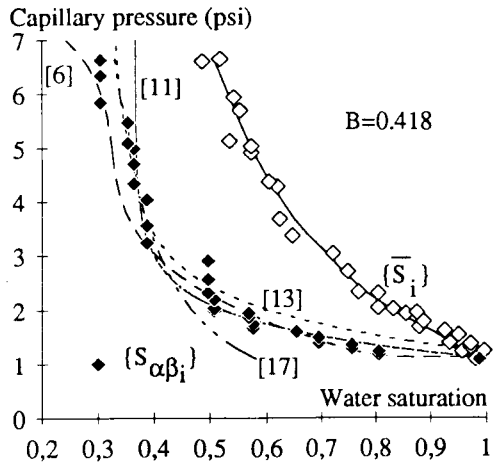

Figure 17 : Interpretation of raw, noisy experimental data (◊) from Bentsen and Anli [11]. The black points represent the corresponding $S_{\alpha\beta}$ solution. Other solutions [6,11,13,17] are given for comparison (Fig. 2).

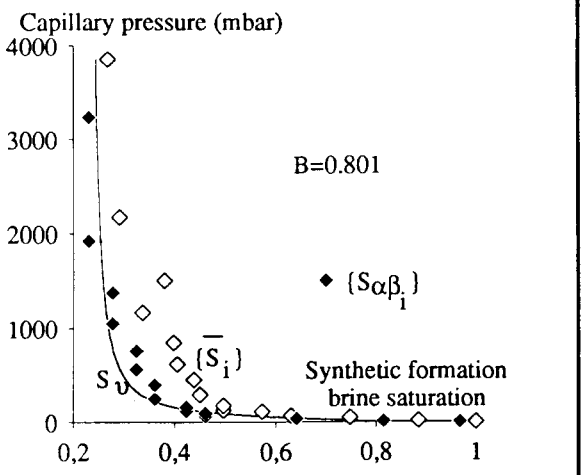

Figure 18 : Interpretation of experimental data (◊) from a North Sea sandstone core (air and synthetic formation brine). The black points depict the $S_{\alpha\beta}$ solution and the continuous line represents the S_υ solution.

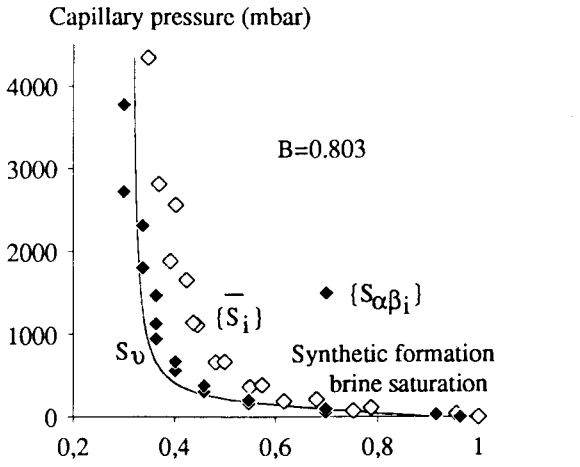

Figure 19: Interpretation of experimental data (◊) from an North Sea sandstone core. The black points depict the $S_{\alpha\beta}$ solution and the curve shows the S_υ solution.

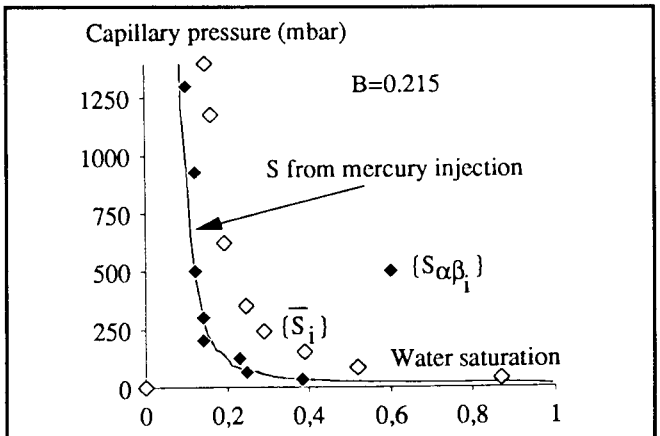

Figure 20 : Interpretation of experimental data (◊) by Glotin et al. ([17], Berea sandstone). The black points depict the $S_{\alpha\beta}$ solution. The curve shows the capillary pressure measured by mercury injection [17].

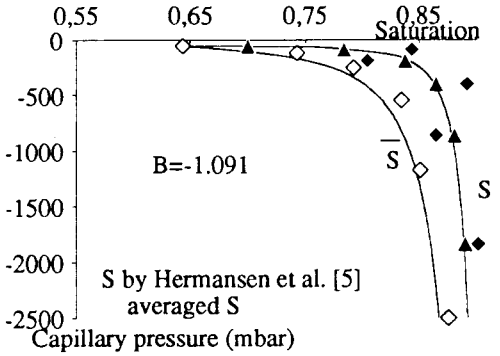

Figure 21 : Imbibition data (◊) from Hermansen et al. [5] (North Sea sandstone). The S(Pc) solution proposed by these authors is shown before averaging (black squares) and after averaging (triangles). The continuous line is a smooth of their averaged solution and the dashed line is the corresponding average saturation according to (3).

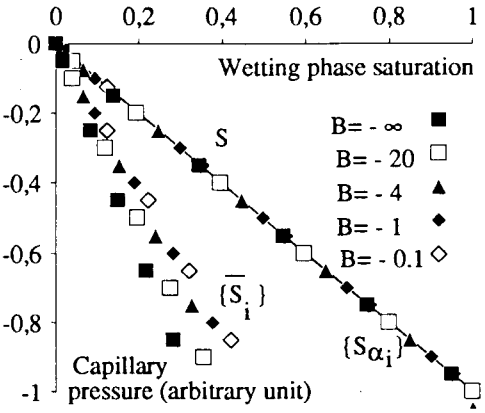

Figure 22 : Interpretation of artificially generated datasets. The left-hand points represent data generated for different B values according to equation (3), for S=-Pc (continuous line). The right-hand points are corresponding S_α sets (see text).

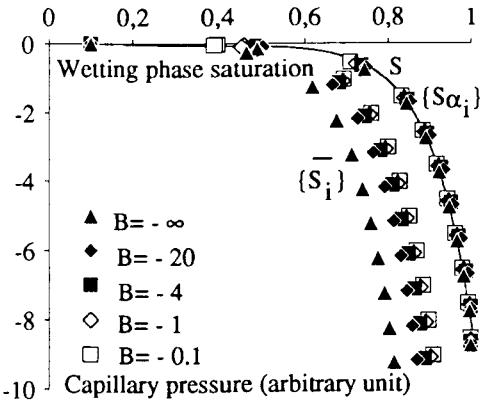

Figure 23 : Interpretation of artificially generated datasets. The left-hand points represent data generated for different B values according to equation (3), for 0≥Pc≥-0.001: S=0.1; Pc<-0.001: S=0.1+0.1Log[-1000 Pc] (line). The right-hand points are corresponding S_α.

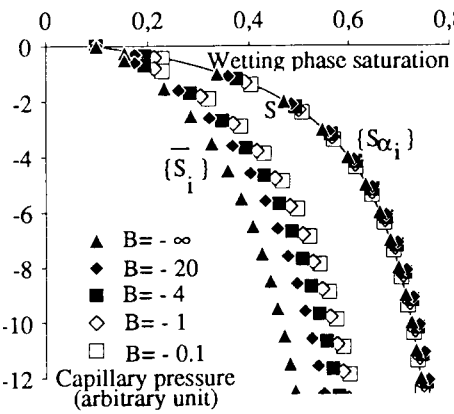

Figure 24 : Interpretation of artificially generated datasets. The left-hand points represent data generated for different B values according to equation (3) for S=0.85+1.5/(Pc-2) (continuous line). The right-hand points are corresponding S_α sets (see text).

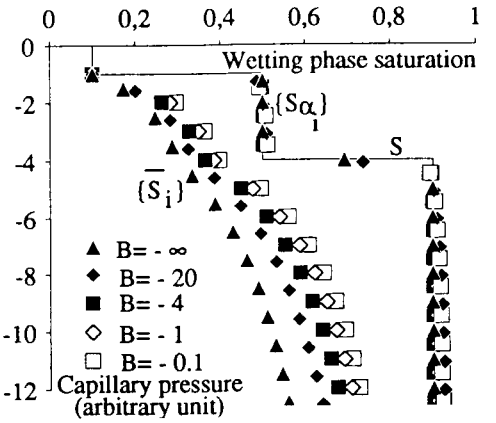

Figure 25 : Interpretation of artificially generated datasets. The left-hand points represent data generated for different B values according to equation (3) for step function 0≥Pc≥-1: S=0.1; -1>Pc≥-4: S=0.5; Pc<-4 : S=0.2 (continuous line). The right-hand points are the corresponding S_α sets (see text).

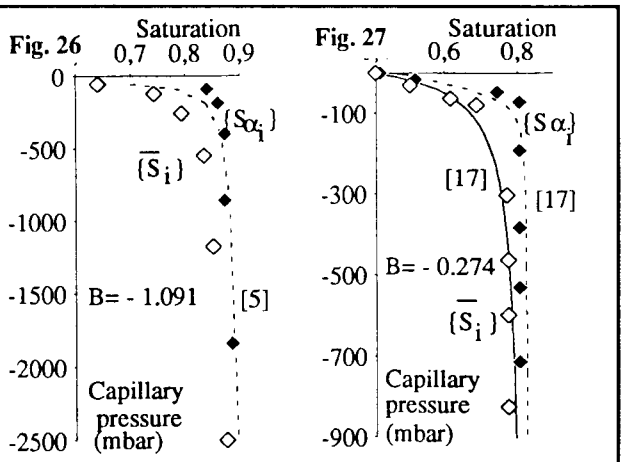

Figure 26 : Imbibition data (◊) from Hermansen et al. [5]. The dashed line is these authors' averaged solution (Fig. 21). The black squares depict the S_α solution.

Figure 27 : Imbibition data (◊) from Glotin et al. [17] (Berea sandstone). The continuous line is the fit used by these authors to obtain capillary pressure curve (dashed line). The black squares depict the S_α solution.

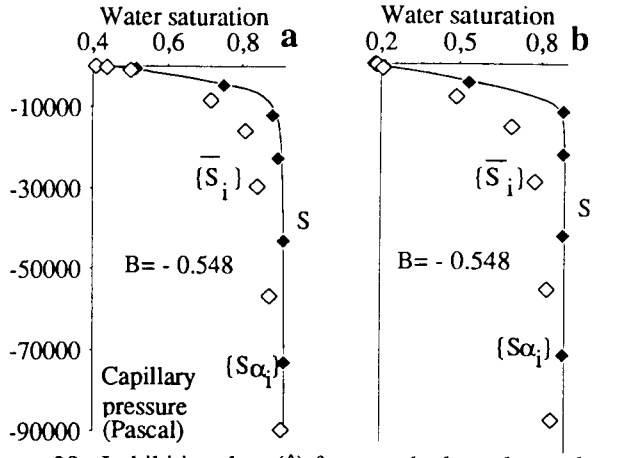

Figure 28 : Imbibition data (◊) from packed-sand samples with intermediate wettability. The lines are the solutions obtained when a Rajan-type approximation [17] is used. The black squares show S_α solutions.

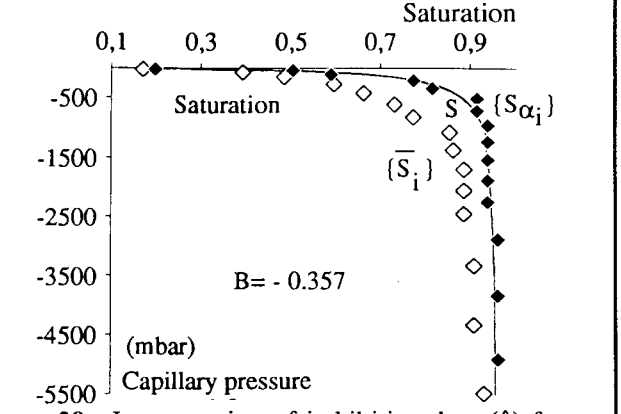

Figure 29 : Interpretation of imbibition data (◊) from a carbonate core sample. The line is the solution obtained when equation (3) is solved with a Rajan approximation [17]. The black squares show the S_α solution.